Characteristics and multi-lineage differentiation of bone marrow mesenchymal stem cells derived from the Tibetan mastiff

SHUANG ZHANG[1], CHENQIONG ZHAO[1], SHI LIU[1], YUFENG WANG[1], YUHUA ZHAO[1], WEIJUN GUAN[2] and ZHIQIANG ZHU[1]

[1]Scientific Research Center, Harbin Sport University, Harbin, Heilongjiang 150008; [2]Institute of Animal Science, Chinese Academy of Agricultural Sciences, Beijing 100193, P.R. China

Received April 14, 2017; Accepted March 13, 2018

DOI: 10.3892/mmr.2018.9172

Abstract. Bone marrow mesenchymal stem cells (BM-MSCs) are pluripotent stem cells that are regarded as ideal resources for the reconstruction of tissues and organs. The Tibetan mastiff is a breed of domesticated Chinese native dog that is well-adjusted to the high-altitude environments of Tibet. To the best of our knowledge, the biological characterization and multi-lineage differentiation of Tibetan mastiff BM-MSCs have not been reported previously. Therefore, the present study aimed to investigate the biological characteristics and therapeutic potential of Tibetan mastiff BM-MSCs. A cell culture system was constructed and cells were cultured to 23 passages *in vitro*. Growth curves and colony formation studies suggested that BM-MSCs had a high self-renewal capacity and that their proliferation rate declined with age. Karyotype analysis demonstrated that BM-MSCs were diploid and genetically stable. Semi-quantitative polymerase chain reaction analysis revealed that BM-MSCs positively expressed cluster of differentiation (CD)73, CD90, CD105, CD166 and vimentin, although they were negative for the endothelial cell marker CD31. Additionally, immunofluorescence staining revealed that the cells expressed CD29, CD44, CD90, CD105 and vimentin. Flow cytometric analysis revealed that the rates of positive expression of vimentin, CD44, CD90 and CD105 were all >97%. BM-MSCs were able to differentiate into adipocytes, osteoblasts, cartilage cells, hepatocytes and functional insulin-secreting cells. In conclusion, Tibetan mastiff BM-MSCs may be purified successfully using a whole bone marrow culture method. The findings of the current study suggested important potential applications of BM-MSCs as a source for regenerative therapies.

Correspondence to: Professor Zhiqiang Zhu, Scientific Research Center, Harbin Sport University, 1 Dacheng Street, Nangang, Harbin, Heilongjiang 150008, P.R. China
E-mail: 13167349687@163.com

Professor Weijun Guan, Institute of Animal Science, Chinese Academy of Agricultural Sciences 2 Yuanmingyuan West Road, Haidian, Beijing 100193, P.R. China
E-mail: weijunguan301@gmail.com

Abbreviations: MSCs, mesenchymal stem cells; BM-MSCs, bone marrow mesenchymal stem cells; DM, diabetes mellitus; IDDM, insulin-dependent DM; NIDDM, non-insulin-dependent DM; PCR, polymerase chain reaction; P4, passage 4; PPAR-γ, peroxisome proliferator-activated receptor-γ; ALB, albumin; AFP, α-fetoprotein; PDX1, pancreatic and duodenal homeobox 1; CFU-F, colony forming unit fibroblast; RUNX2, runt-related transcription factor 2; SPP1, secreted phosphoprotein 1; ITS, insulin-transferrin selenium

Key words: Tibetan mastiff, bone marrow mesenchymal stem cells, biological characteristics, liver injury, diabetes

Introduction

Stem and progenitor cells have been identified as major contributors to the development, homeostasis nd repair of tissues and organs (1-3). Tissue damage triggers the secretion of immunomodulatory and trophic factors from stem cells, supporting the repair process (4). Among the numerous adult stem/progenitor cells, mesenchymal stem cells (MSCs) exhibit great potential for use in numerous medical applications (5). MSCs exhibit adherent growth, a fibroblast-like shape, and a capacity for self-renewal and differentiation into numerous cell types, including all three germ layers (6-8). Among the various types of MSCs, bone marrow MSCs (BM-MSCs), which are pluripotent progenitor cells, are deemed to be able to influence natural immune function (9), the inhibition of local inflammatory responses (10) and sepsis (11,12). Although a number of studies on BM-MSCs derived from various species, including human (13), rat (14), rabbit (15), sheep (16), chicken (17) and bovine (18) species, have been performed, there have been no reports, to the best of our knowledge, on Tibetan mastiff-derived BM-MSCs. Therefore, the characterization of BM-MSCs from the Tibetan mastiff has not yet been performed.

The Tibetan mastiff is one of the oldest dog breeds in the world, and has been domesticated and introduced into many other countries as a pet (19). The Tibetan mastiff has adjusted to survival at high altitudes (typically 4,500 m above sea level) (20). As the Tibetan mastiff has an enhanced metabolic capacity, it is able to grow a healthy body and maintain good physiological functioning even at high elevations (21). Tibetan mastiffs have been a common breed in the Qinghai-Tibet

Plateau for thousands of years (22), and are predominantly found in the Sichuan, Qinghai and Tibet regions in China. Tibetan mastiffs share a number of prevalent diseases, including diabetes, heart disease, liver injury, blindness, deafness, heart disease and epilepsy, with humans (23). As this breed has evolved as a pet, it has become necessary to find effective treatments for the diseases that may become a threat to the health of Tibetan mastiffs (23).

The liver is a key metabolic organ in humans and other animal species, and end-stage liver disease is a condition that is frequently accompanied by serious complications, in addition to endangering life (24). Infectious canine hepatitis is a common disease that is caused by canine adenovirus type-1. This virus may infect numerous organs, and most frequently attacks the liver, causing hepatitis. The clinical symptoms of infectious canine hepatitis include thirst, loss of appetite, tonsillitis, hepatomegaly and abdominal tenderness, and animals may additionally have conjunctivitis, photophobia and increased eye secretions. In addition, as the virus multiplies within the iris and ciliary body and causes corneal edema and opacity, 'blue eyes' is frequently observed with this disease. The virus may be contracted via direct contact with contaminated urine, feces or other fluids from an infected dog, and may affect dogs of all ages and breeds (25). Injection of hepatocyte-like cells has been demonstrated to be a highly effective treatment for liver injury (26). BM-MSCs differentiate into functional hepatocyte-like cells, and may therefore be an attractive basis for novel therapies for liver diseases.

Diabetes mellitus (DM) is one of the most common endocrine and metabolic diseases in canines. DM primarily occurs in older dogs, and its prevalence is rising year by year. The estimated prevalence of diabetes in canines is 1/2,000 to 1/66. In domestic dogs, the typical age of onset is 7-9 years and the prevalence is 0.1-0.6%; it is approximately three times more prevalent in female dogs compared with male dogs, with the highest prevalence in obese dogs aged >5 years (27). There is no internationally recognized standard for the classification of canine and feline diabetes; however, canine diabetes may be divided into insulin-dependent and insulin-independent classes (28). DM is a metabolic disorder that causes hyperglycemia, and it has been demonstrated to influence the metabolism of carbohydrates, lipids and proteins (29). Additionally, DM is an endocrine disorder that affects the immune system (30). An effective cure for diabetes is urgently required. A number of studies have demonstrated that BM-MSCs may be differentiated into functional insulin-secreting cells *in vitro*, highlighting their therapeutic potential for the treatment of diabetes.

In the present study, a culture of Tibetan mastiff BM-MSCs was established, and differentiation of the cells into three different germ layers was induced. Furthermore, the function of induced liver cells and insulin-secreting cells was determined, thereby demonstrating the preparation of BM-MSCs for the treatment of various diseases. Their biological characteristics with respect to growth kinetics and surface antigen expression were additionally investigated. The present study may provide a basis for the examination of Tibetan mastiff-derived BM-MSCs and may provide a novel direction for the development of treatments for certain canine diseases.

Materials and methods

Experimental animals. A total of two male Tibetan mastiffs (1 day old; weight, 480 g) were provided by the Beijing Tibetan Mastiff breeding base (Beijing, China) and maintained at a temperature of 22˚C under a 12-h light/dark cycle and had free access to food and water. Animal experimental procedures were consistent with the Institutional Animal Care guidelines. The present study was approved by the Institute of Animal Science, Chinese Academy of Agricultural Sciences (Beijing, China).

Isolation, culture, and purification of BM-MSCs. BM-MSCs were purified and cultured according to a previously published culture system for BM-MSCs (31). Tibetan mastiff bone marrow samples were isolated from femoral and tibial fractures. The bone marrow was washed three times with low-glucose Dulbecco's modified Eagle's medium (L-DMEM; Gibco; Thermo Fisher Scientific, Inc., Waltham, MA, USA) supplemented with 1% penicillin/streptomycin. The cell infusion was centrifuged at 250 x g for 10 min, the supernatant was discarded, and the pellet resuspended in complete medium consisting of 90% (v/v) L-DMEM, 10% (v/v) fetal bovine serum (FBS; Gibco; Thermo Fisher Scientific, Inc.), 1% (v/v) L-glutamine and 10 ng/ml fibroblast growth factor (FGF)-β (PeproTech, Inc., Rocky Hill, NJ, USA). The cells were seeded into a culture plate at $1x10^5$ cells/ml and incubated at 37˚C in an incubator with 5% CO_2.

Immunofluorescence analysis of BM-MSC surface markers. BM-MSCs were fixed with 4% (w/v) paraformaldehyde at 4˚C for 30 min and permeabilized with 0.25% (v/v) Triton X-100 at room temperature for 15 min. BM-MSCs were subsequently blocked in 10% (v/v) goat serum (BIOSS, Beijing, China) at room temperature for 60 min and incubated with the following antibodies: Anti-CD29 (cat. no. bs-20631R; 1:200); anti-CD44 (cat. no. bs-0521R; 1:200), anti-CD90 (cat. no. bs-0778R; 1:200); anti-CD105 (cat. no. bs-0579R; 1:200); anti-vimentin (cat. no. bs-8533R; 1:200; all from BIOSS); anti-ALB (cat. no. ab83465; 1:200). Subsequently, cells were incubated with fluorescein isothiocyanate (FITC)-conjugated goat anti-rabbit secondary antibodies (cat. no. ZF-0311; 1:200; OriGene Technologies, Inc., Beijing, China) at room temperature. Finally, cells were counterstained with DAPI (Sigma-Aldrich; Merck KGaA, Darmstadt, Germany). Images were captured using a Nikon TE-2000-E confocal microscope with an attached Nikon ZE-1-C1 3.70 digital camera system (Nikon Corporation, Tokyo, Japan).

Semi-quantitative-polymerase chain reaction (PCR). Total RNA was extracted from cells using TRIzol reagent (Invitrogen; Thermo Fisher Scientific, Inc.), and reverse transcribed into cDNA using a Reverse Transcription kit (Takara Biotechnology Co., Ltd., Dalian, China). cDNA was amplified by PCR using specific primers, with GAPDH as an internal control (Table I). The reaction conditions consisted of an initial denaturation step at 94˚C for 5 min, followed by 30 cycles at 94˚C for 30 sec, 55-60˚C for 30 sec and 72˚C for 30 sec, and a fnal cycle at 72˚C for 10 min. The products were visualized on 2% agarose gels with ethidium bromide.

Table I. Primer sequences used for reverse transcription-polymerase chain reaction.

Gene	Primer sequences	Tm (˚C)	Product length (bp)
RUNX2	F:5'-TTCCAGAATGCTTCCGCCAT-3'	60	343
	R:5'-CCCTCTCGTGGTTGCAAGAT-3'		
SPP1	F:5'-GCCAAGCAAGTCCAACGAAA-3'	59	344
	R:5'-CCACATGTGACGTGAGGTCT-3'		
LPL	F:5'-ACTGGTTGGCGGAGGAATTT-3'	60	469
	R:5'-GCTTCCTTTGAGTTGCACCG-3'		
PPAR	F:5'-TTTCCCATTGCCGCTCAAGT-3'	60	262
	R:5'-GCAAATCGGGCTTTCTGTGT-3'		
COL2A1	F:5'-AATTGCTGGCTTCAAAGGCG-3'	58	353
	R:5'-GACCGACTTTGCCTTGAGGA-3'		
SOX9	F:5'-CCGAACAGACGCACATTTCC-3'	60	302
	R:5'-TTCGTTGACGTCGAAGGTCT-3'		
AFP	F:5'-CCGTCACCAGTTGTAAGGCA-3'	60	290
	R:5'-AACCGTTATGGCTCGGAAGG-3'		
ALB	F:5'-AGCCTTTGGCACAATGAAGT-3'	59	170
	R:5'-GAGAAAAGGCAACCAGCACC-3'		445
Insulin	F:5'-CCTTCGTTAACCAGCACCTGT-3'	58	
	R:5'-CAGCTGGTAGAGGGAGCAGAT-3'		
Nestin	F:5'-TCCGGGAAGGAGTCTGTAGG-3'	59	267
	R:5'-ACCCTCTGGGGACTCATCTC-3'		
CD73	F:5'-CACATCTGATGATGGGCGGA-3'	60	460
	R:5'-GGTTTCCCCAAAGGGCAGTA-3'		
CD90	F:5'-TGGAGGGTTGGAGAAGGAGT-3'	60	265
	R:5'-GCACTGATGGGGGAGGTAAG-3'		
CD105	F:5'-GAGCCCAGTGACTCTTTCCC-3'	58	377
	R:5'-AAACGTCACCTCACCCCTTG-3'		
CD166	F:5'-GACCAAGCAGATTGGCGATG-3'	58	495
	R:5'-TCTCTGTTTTCATTAGCAGAGACAT-3'		
CD31	F:5'-ACCCCTATTGTGCTATGTCAGT-3'	59	212
	R:5'-AGGCATGGTGATTAAGCCCT-3'		
GAPDH	F:5'-TTCACCACCATGGAGAAGGC-3'	60	497
	R:5'-TCCGATGCCTGCTTCACTAC-3'		

RUNX2, runt-related transcription factor 2; SPP1, secreted phosphoprotein 1; LPL, lipoprotein lipase; PPAR, peroxisome proliferator-activated receptor; COL2A1, collagen type II α1 chain; SOX9, SRY-box 9; AFP, α-fetoprotein; ALB, albumin; CD, cluster of differentiation.

Flow cytometric analysis. To detect the levels of vimentin, CD44, CD90 and CD105, the present study characterized passage 8 cells by fluorescence-activated cell sorting. In brief, cells were detached with trypsin, fixed with 70% precooling ethyl alcohol overnight at 4˚C and incubated with monoclonal antibodies anti-CD44 (cat. no. bs-0521R; 1:200), anti-CD90 (cat. no. bs-0778R; 1:200), anti-CD105 (cat. no. bs-0579R; 1:200) and anti-vimentin (cat. no. bs-8533R; 1:200; all from BIOSS). Cells were subsequently stained with FITC-conjugated goat anti-rabbit secondary antibodies (cat. no. ZF-0311; 1:200; OriGene Technologies, Inc., Beijing, China). For the negative control, the cells were incubated with PBS instead. Secondary antibodies were omitted. Cells were evaluated by the FC500 flow cytometer (BD Biosciences, Franklin Lakes, NJ, CA, USA). The mean fluorescence intensity was determined with Windows FCS Express version 3 (De Novo Software, Glendale, CA, USA).

Growth curve assay. The growth curves of BM-MSCs at passage (P)4, 12 and 21 were determined. Cells ($1x10^4$) were inoculated into each well of a 24-well plate. Cells were selected from three random wells to count using a hemocytometer each day, and growth curves were constructed based on the mean values. The population doubling times were calculated for 8 days according to the growth curves.

Karyotype and chromosome analysis. Chromosomes were prepared and analyzed according to standard methods (32). Following Giemsa staining, the numbers of chromosomes were calculated and analyzed according to previously described protocols (33,34).

Colony-forming unit fibroblast (CFU-F) assay. To assess clonogenic potential, cells were plated at a low

density (100 cells/cm^2) and cultured in complete medium at 37˚C for 2 weeks. The medium was replaced twice per week. CFU-F analysis was conducted after ~10 days culture. Colony-forming units were stained by Giemsa (1:10) at room temperature according to the manufacturer's protocols and counted under the light microscope. The colony-forming rate was formulated as colony-forming unit numbers/starting cell number per 24-well x100%.

Differentiation potential of BM-MSCs. For osteogenic differentiation of BM-MSCs, when BM-MSCs reached 70% confluence the culture medium was replaced with a medium composed of L-DMEM, 10% FBS, 100 nM dexamethasone, 10 mM β-glycerophosphate and 250 mM L-ascorbic acid. Cells cultured without dexamethasone, β-glycerophosphate (all Sigma-Aldrich; Merck KGaA) and L-ascorbic acid were used as a control. Cells were cultured for 22 days and the mediumwas replaced three times per week. Cells were fixed with 4% paraformaldehyde for 30 min at room temperature and stained with 0.1% Alizarin Red S (cat. no. A5533; Sigma-Aldrich; Merck KGaA) at room temperature according to the manufacturer's protocols when obvious calcium deposits appeared. The osteoblast-specific genes secreted phosphoprotein 1 (SPP1) and runt-related transcription factor 2 (RUNX2) were detected in the cells using semi-quantitative PCR (Table I).

For adipogenic differentiation of BM-MSCs, BM-MSCs in 6-well plates at a density of 2x10^5 cells/well were divided into an induced group and control group. Upon reaching 70% confluence, the induced group cells were incubated in adipocyte-inducing medium composed of L-DMEM, 10% FBS, 1.0 mmol/l dexamethasone, 0.5 mmol/l isobutyl-methylxanthine and 10 mg/l insulin (all Sigma-Aldrich; Merck KGaA) for 12 days. Control group cells were cultured in the same way without inducers. Cells were stained with 0.3% Oil Red O (cat. no. O8018; Beijing Solarbio Science & Technology Co., Ltd., Beijing, China) at room temperature according to the manufacturer's protocols, and adipocyte-specific genes [peroxisome proliferator-activated receptor-γ (PPAR-γ) and lipoprotein lipase (LPL)] were detected in cells by semi-quantitative PCR.

For chondrogenic differentiation of BM-MSCs, BM-MSCs were divided into an induced group and control group. Upon reaching 70% confluence, the culture medium of the induced group was replaced with chondrocyte-inducing medium consisting of DMEM/F12, 5% FBS, 1% insulin-transferrin selenium (ITS), 40 mg/ml L-proline, 39 ng/ml dexamethasone, 100 mg/ml sodium pyruvate, 50 mg/ml L-ascorbic acid, and 10 ng/ml transforming growth factor-β3. Control group cells were cultured in the same way without inducers. Cells were cultured with medium for three weeks and the medium was changed three times per week. Chondrocytes were identified by Alcian blue (cat. no. G2541; 1:100; Beijing Solarbio Science & Technology Co., Ltd.) staining at room temperature according to the manufacturer's protocols and semi-quantitative PCR analysis of chondrocyte-specific genes [collagen type II α1 chain (COL2A1) and SRY-box 9 (SOX9)].

For hepatocyte differentiation of BM-MSCs, BM-MSCs were divided into an induced group and a control group. Upon reaching 50% confluence, the culture medium of the induced group was replaced with a hepatocyte-inducing medium comprising L-DMEM, 5% FBS, 40 nmol/ml dexamethasone, 20 ng/ml FGF-4, 20 ng/ml HGF and 1% ITS (Sigma-Aldrich; Merck KGaA). Cells cultured without any inducers were used as the control group. Cells were cultured with medium for two weeks. The mediumwas changed three times per week. Periodic acid-Schiff (PAS; cat. no. G1360; Beijing Solarbio Science & Technology Co., Ltd.) staining at room temperature was used to detect glycogen according to the manufacturer's protocols. Hepatocyte-specific genes were detected via semi-quantitative PCR [albumin (ALB) and α-fetoprotein (AFP)] and immunofluorescence analysis (ALB).

For functional β-like cell differentiation, a three-step approach to induce the differentiation of BM-MSCs into insulin-secreting cells was used. In the first step, the cells were cultured with high-glucose DMEM, 10% FBS and 10^{-6} mol/l retinoic acid (Sigma-Aldrich; Merck KGaA) for 24 h. The medium was subsequently replaced, in the second step, with a different medium composed of L-DMEM, 10% FBS, 10 mmol/l nicotinamide (Sigma-Aldrich; Merck KGaA), 20 ng/ml epidermal growth factor (PeproTech, Inc.), 50 ng/ml FGF-10 (R&D Systems, Inc., Minneapolis, MN, USA) and 300 nmol/l (-)-indolactam V (LC Laboratories, Woburn, MA, USA) for 1 week. In the third stage, cells were treated with L-DMEM, 10% FBS, 10 nmol/l exendin-4 (Sigma-Aldrich; Merck KGaA) and 50 ng/ml activin A (PeproTech, Inc.) for 1 week. The medium was replaced three times per week. Control cells were treated with L-DMEM without the following inducers: Retinoic acid, nicotinamide, epidermal growth factor, FGF-10, indolactam V, exendin-4 and activin A.

Insulin-secreting cell induction was detected by morphological observation under the light microscope, positive staining with dithizone (1:10) (35), immunofluorescence [for pancreatic and duodenal homeobox 1 (PDX-1), insulin (INS), nestin (NES) and C-peptide] and semi-quantitative PCR (for INS and NES expression). To detect the secretion of insulin for 5.5 and 25.5 mM concentrations of glucose, an ELISA (EMINS; Invitrogen; Thermo Fisher Scientific, Inc.) was used.

Statistical analysis. GraphPad Prism software version 6 (GraphPad Software, Inc., La Jolla, CA, USA) was used to analyze the data by Student's t-test. Data from three sets of results were expressed as the mean ± standard deviation. $P<0.05$ was considered to indicate a statistically significant difference.

Results

Morphological characteristics of BM-MSCs. After 6 h seeding, cells began to attach and proliferate. Although hemocytes were initially present among the BM-MSCs, these were eliminated after sub-culture (Fig. 1). Adherent cells formed a fibroblast-like layer, and the appearance of the cells remained the same for all passages. The cells grew until P23, following which they appeared to enter a senescent phase (Fig. 1).

Surface markers of BM-MSCs. Immunofluorescence, semi-quantitative PCR and flow cytometry were used to analyze the surface markers of BM-MSCs. Cells from P4, P10 and P18 exhibited positive expression levels of CD73,

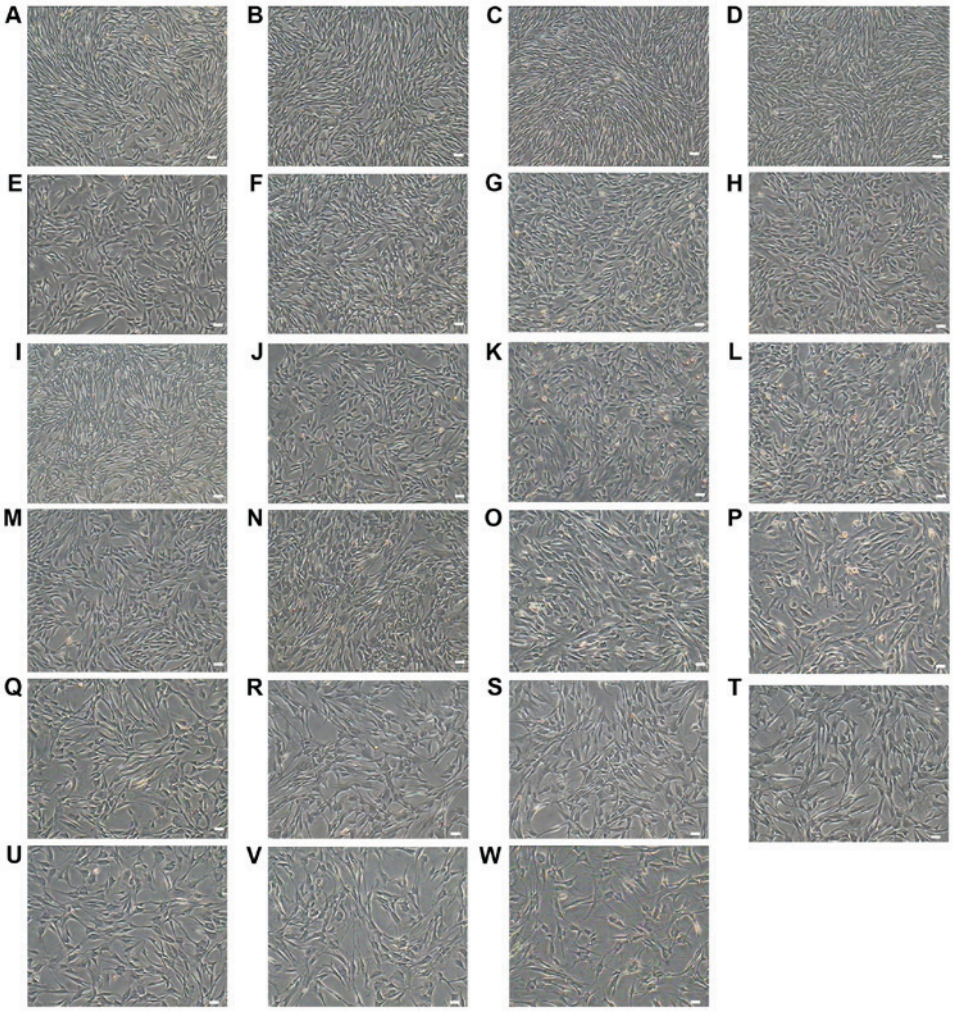

Figure 1. Morphology of cultured BM-MSCs. (A) Passage 1, (B) Passage 2, (C) Passage 3, (D) Passage 4, (E) Passage 5, (F) Passage 6, (G) Passage 7, (H) Passage 8, (I) Passage 9, (J) Passage 10, (K) Passage 11, (L) Passage 12, (M) Passage 13, (N) Passage 14, (O) Passage 15, (P) Passage 16, (Q) Passage 17, (R) Passage 18, (S) Passage 19, (T) Passage 20, (U) Passage 21, (V) Passage 22 and (W) Passage 23, respectively (scale bar, 100 μm). All cells were homogeneous and exhibited a spindle-shaped morphology during culture. BM-MSCs, bone marrow mesenchymal stem cells.

CD90, CD105, CD166 and CD31 upon semi-quantitative PCR analysis; this was not the case for CD31 (Fig. 2). As presented in Fig. 3, immunofluorescence staining revealed that BM-MSCs expressed the specific markers CD29, CD44, CD90, CD105 and Vimentin. Additionally, flow cytometric analysis revealed high rates of positive expression of the following markers: Vimentin (99.70%), CD44 (99.07%), CD90 (99.86%) and CD105 (99.87%) (Fig. 4). Data are presented as the mean ± standard deviation.

Colony formation and growth kinetics. Clonogenic capacity was assessed by microscopy (Fig. 5Aa-c). The number of colonies formed by P4, P12 and P21 cells was 38.8±0.4, 28.6±0.2 and 24.6±0.3, respectively (Fig. 5Ad). These results suggested that the BM-MSCs were capable of self-renewal. Data are presented as the mean ± standard deviation.

Growth curves demonstrated that P4, P12 and P21 cells exhibited similar growth and proliferation kinetics (Fig. 5B). Following a 3-day latency phase, cells reached a logarithmic phase, and subsequently a stable phase. The population doubling times were 36.3, 41.6 and 45.8 h for P4, P12 and P21, respectively (data not shown).

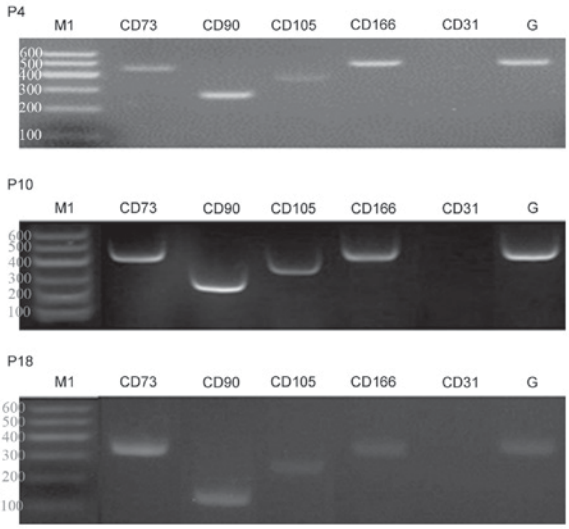

Figure 2. Semi-quantitative polymerase chain reaction analysis of specific markers in BM-MSCs. The results demonstrated that BM-MSCs of different passages all expressed CD73, CD90, CD105 and CD166, and did not express CD31 (an endothelial cell marker). GAPDH was used as an internal control. CD, cluster of differentiation; BM-MSCs, bone marrow mesenchymal stem cells; G, GAPDH; M1, Marker 1; molecular ladder; P, passage.

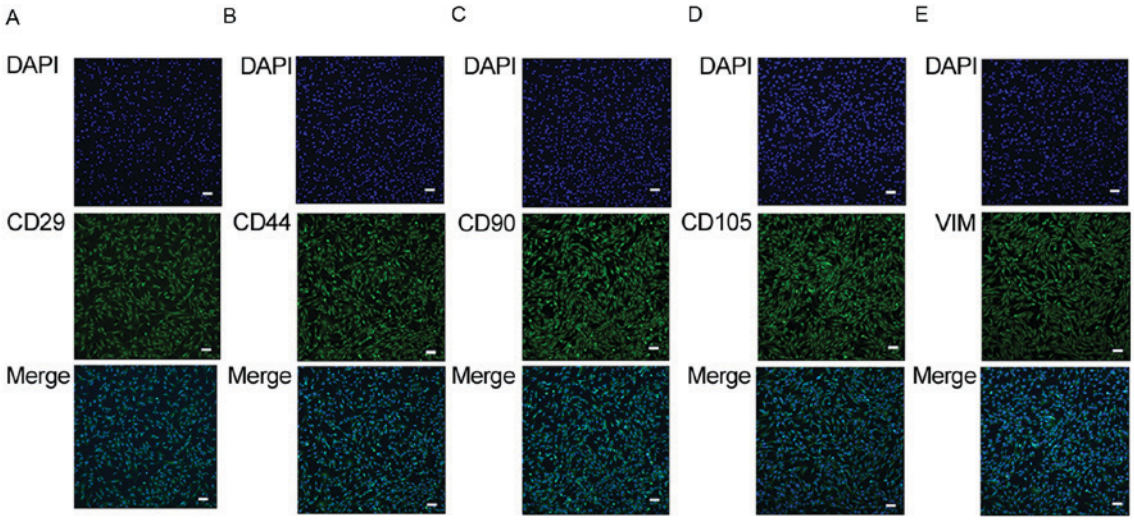

Figure 3. Immunofluorescence staining of BM-MSCs at passage 5. The immunofluorescence staining images illustrated markers of the BM-MSC phenotype. Cells expressed (A) CD29, (B) CD44, (C) CD90, (D) CD105 and (E) VIM. Scale bar, 100 μm. CD, cluster of differentiation; VIM, vimentin; BM-MSCs, bone marrow mesenchymal stem cells.

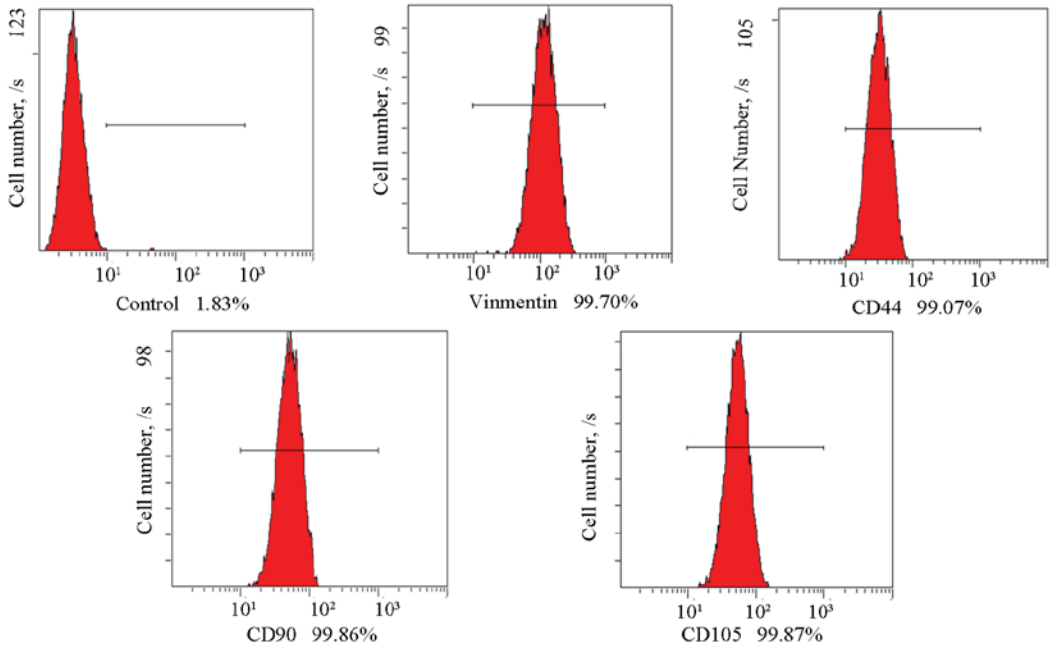

Figure 4. Flow cytometric detection of BM-MSCs. BM-MSCs were labelled for the MSC surface makers Vimentin, CD44, CD90 and CD105. The control sample was cells incubated with PBS and no antibodies. The rates of cells positively expressing each marker were all >96%. Data are presented as the mean ± standard deviation. CD, cluster of differentiation; VIM, vimentin; BM-MSCs, bone marrow mesenchymal stem cells.

Karyotype analysis. BM-MSCs were diploid, containing 78 chromosomes (38 pairs of euchromosomes and two sex chromosomes; Fig. 6). No abnormalities were detected. This result suggested that the cells were stable *in vitro*.

Osteogenic differentiation of BM-MSCs. Following culture with osteogenic inducers, BM-MSCs exhibited significant alterations in appearance (Fig. 7). As time progressed, the morphology of certain BM-MSCs altered, with the cells becoming larger and more polygonal (Fig. 7A). At 4 weeks post-induction, the morphology and positive Alizarin Red S staining were observed (Fig. 7B and C). The number of cell aggregates increased, and semi-quantitative PCR revealed that RUNX2 and SPP1 were expressed in the induced cells, although not in the non-induced control group (Fig. 7D).

Adipogenic differentiation of BM-MSCs. Adipogenic induction of BM-MSCs was detected by Oil Red O staining and semi-quantitative PCR. On day 21, the cells had differentiated into adipocytes successfully (Fig. 8A), and certain cells exhibited positive staining with Oil Red O, where fat droplets were more evident (Fig. 8B). There were no apparent morphological alterations in the control group (Fig. 8C). Semi-quantitative PCR revealed that the induced cells expressed PPAR-γ and LPL on day 21, whereas the control group did not (Fig. 8D).

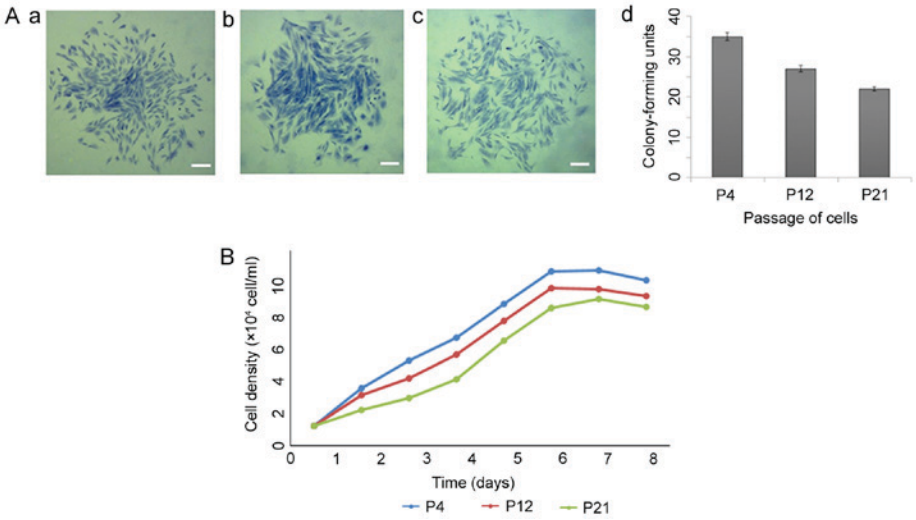

Figure 5. Colony formation assay and growth kinetics. (A) Colonies of BM-MSCs at different passages (scale bar=100 μm): (a) P4; (b) P12 (c) P21 and (d) bar chart of colony-formation rates for different passages of BM-MSCs. (B) P4, P12 and P21 BM-MSCs all had typical sigmoidal growth curves. Cell density is shown by the vertical axis. The growth curves comprised a latent phase, logarithmic phase and plateau phase. Data are presented as the mean ± standard deviation. CD, cluster of differentiation; BM-MSCs, bone marrow mesenchymal stem cells; P, passage.

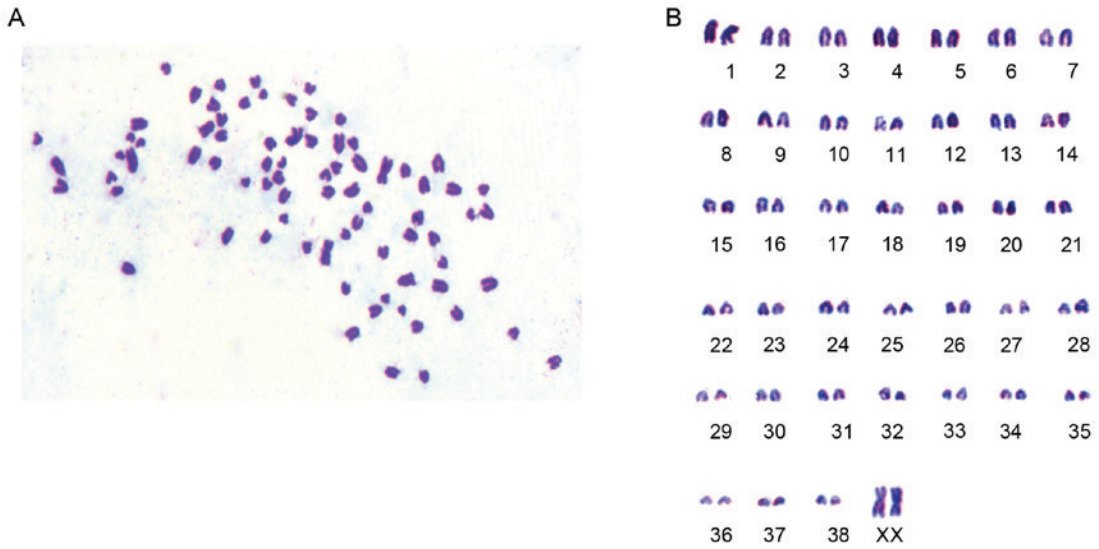

Figure 6. Chromosome and karyotype analysis. (A) Metaphase chromosome analysis (magnification, x1,000) and (B) karyotype analysis of BM-MSCs. The number of chromosomes in the BM-MSCs was 2n=78 [38 pairs of euchromosomes plus two sex chromosomes (XX)]. BM-MSCs, bone marrow mesenchymal stem cells.

Chondrogenic differentiation of BM-MSCs. Following 1 week of incubation in chondrocyte-inducing medium, BM-MSCs appeared to form aggregates and exhibited rapid proliferation. Subsequently, the proliferation rate reduced, and the cells exhibited a higher ratio of nucleus to cytoplasm. Following culture with the chondrogenesis inducers for 4 weeks, the cells exhibited positive staining with Alcian blue (Fig. 9A-C), and the chondrocyte-specific genes COL2A1 and SOX9 were detected by semi-quantitative-PCR (Fig. 9D); however, these genes were not expressed in the control group.

Hepatogenic differentiation of BM-MSCs. Following culture in hepatocyte-inducing medium for 1 week, BM-MSCs exhibited round and polygonal morphology. The numbers of round and polygonal cells increased gradually, and a cobblestone-like morphology appeared 10 days subsequently (Fig. 10Aa). Glycogen synthesis and storage were detected by PAS staining in the induced cells (Fig. 10Ab). By comparison, the control cells exhibited no obvious alterations (Fig. 10Ac). Semi-quantitative PCR revealed that the hepatocyte-specific genes ALB and AFP were expressed in the induced group and not in the control group (Fig. 10B). The induction was additionally evaluated by flow cytometry (Fig. 10C). Based on ALB expression, ~82.65% cells were successfully induced to differentiate into hepatocytes. Data are presented as the mean ± standard deviation. Consistently, immunofluorescence staining and microscopy additionally indicated that the induced cells were positive for ALB (Fig. 10D).

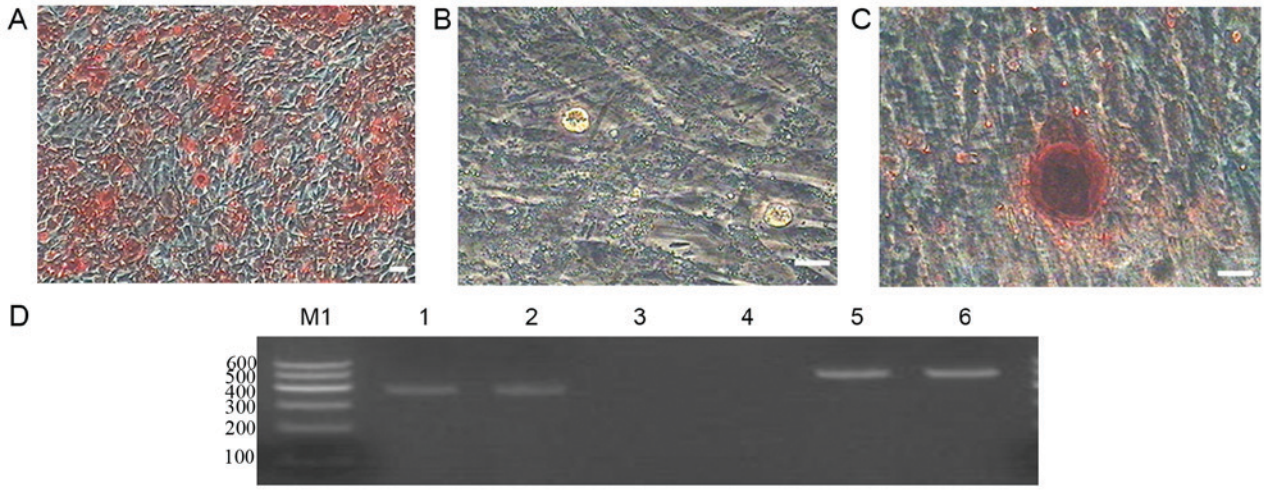

Figure 7. Osteogenic induction of BM-MSCs. Morphological analysis of the osteogenic induction of BM-MSCs was performed. The cells were incubated in inducing medium for 4 weeks. Following induction, cells were positively stained with Alizarin Red S: (A) x40 magnification; (B) x40 magnification; and (C) x200 magnification. (D) Semi-quantitative-polymerase chain reaction analysis of osteoblast-specific genes. The induced group expressed the osteogenic-specific genes RUNX2 (lane 1) and SPP1 (lane 2), whereas the control group (lanes 3 and 4) did not. Lanes 5 and 6 were GAPDH for inducted group and control group, respectively. BM-MSCs, bone marrow mesenchymal stem cells; RUNX2, runt related transcription factor 2; SPP1, secreted phosphoprotein 1; M1, Marker 1; molecular ladder.

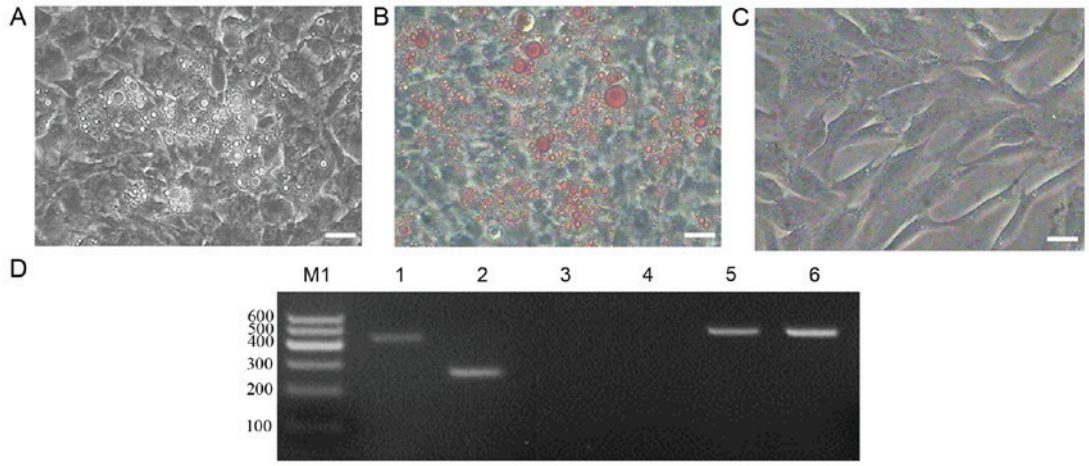

Figure 8. Adipogenic induction of BM-MSCs. (A) Following 21 days of incubation in adipogenic medium, the cells exhibited large fat droplets and (B) were positively stained with Oil Red O. (C) There were no apparent morphological alterations in the control group. Images were captured at magnification, x200. (D) Semi-quantitative polymerase chain reaction analysis demonstrated that the induced group expressed the adipocyte-specific genes LPL (Lane 1) and PPAR-γ (Lane 2), whereas the control group (Lanes 3 and 4) did not. Lanes 5 and 6 were GAPDH for inducted group and control group, respectively. BM-MSCs, bone marrow mesenchymal stem cells; LPL, lipoprotein lipase; PPAR-γ, peroxisome proliferator-activated receptor-γ; M1, Marker 1; molecular ladder.

Insulin-producing β-like cell differentiation. No morphological alterations were observed following step one. Following step two, islet-like clusters began to appear, and these clusters matured following step three. The clusters exhibited scarlet staining with dithizone (Fig. 11A). Semi-quantitative PCR demonstrated that the induced group expressed β-cell-specific genes, including and NES, whereas the control group did not express these genes (Fig. 11B). The ability of the cells to secrete insulin and C-peptide was tested by ELISA *in vitro* at 5.5 and 25.5 mM glucose. The results demonstrated that the induced insulin-secreting cells were functional and glucose-responsive (Fig. 11C).

Specific markers of insulin-secreting cells, including PDX-1, INS, NES and C-peptide, were additionally demonstrated to be expressed using immunofluorescence at different times during induction (Fig. 12).

Discussion

Hematopoietic stem cells (HSCs) and MSCs are the two primary cell types in the bone marrow. HSCs are recognized as blood cell precursors, whereas MSCs are capable of multipotent differentiation, self-renewal and expansion. Stable and uniform BM-MSCs may be separated from HSCs of the bone marrow via the adherence screening method, density gradient centrifugation, fluorescence-activated cell sorting (31) and immunomagnetic microbead selection (32,33).

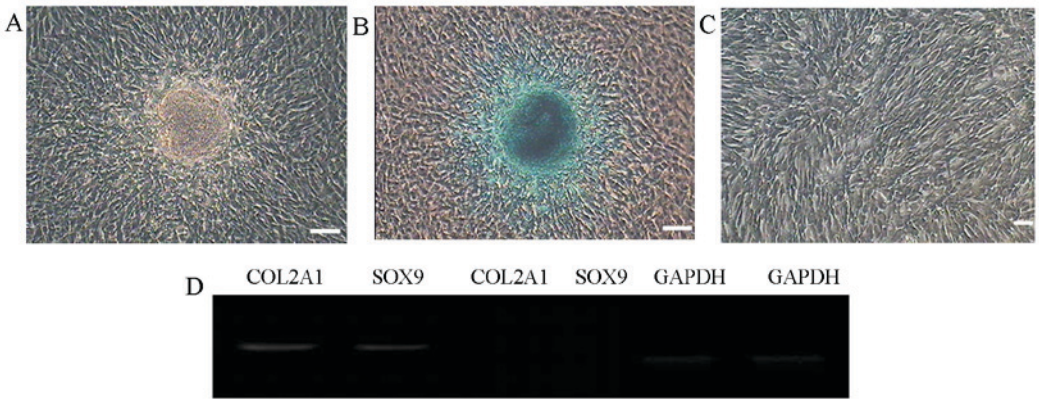

Figure 9. Chondrogenic induction of BM-MSCs. Following incubation in chondrogenic induction medium for 4 weeks, the cells (A) formed cluster-like aggregates and (B) were positive for Alcian blue staining. (C) There were no apparent morphological alterations in the control group. Images were captured at magnification, x40. (D) The results of the semi-quantitative polymerase chain reaction revealed expression of the chondrocyte-specific genes COL2A1 and SOX9 in induced cells, although not in control cells. BM-MSCs, bone marrow mesenchymal stem cells; COL2A1, collagen type II α1 chain; SOX9, SRY-box 9.

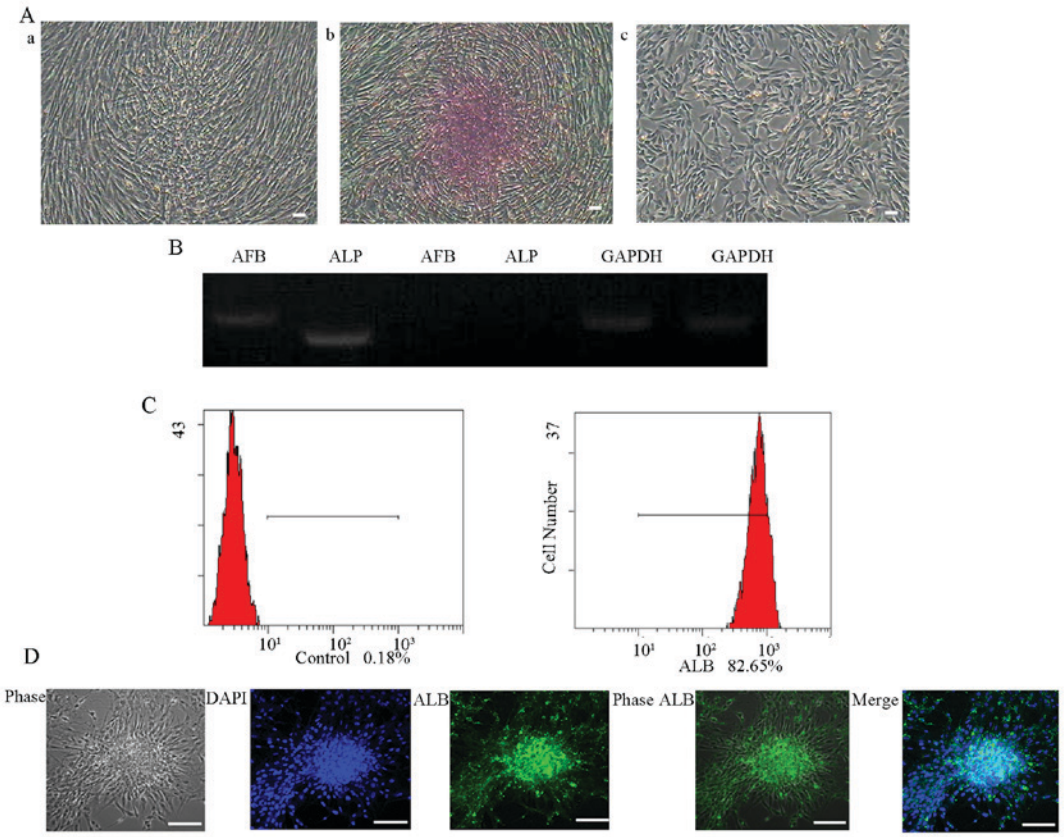

Figure 10. Hepatocyte differentiation of BM-MSCs. (A) Cellular morphologies and PAS staining: (a) Pre-staining, (b) PAS staining and (c) control group cells without PAS staining. Images were captured at magnification, x40. (B) Semi-quantitative polymerase chain reaction analysis demonstrated the expression of the hepatocyte-specific genes AFP and ALB in induced cells, although not in control cells. (C) Flow cytometric analysis of ALB expression demonstrated the induction of BM-MSCs: Control group and induced group. Data are presented as the mean ± standard deviation. (D) Immunofluorescence revealed that the cells were positive for ALB. BM-MSCs, bone marrow mesenchymal stem cells; PAS, periodic acid-Schiff; AFP, α-fetoprotein; ALB, albumin.

Cells isolated from the bone marrow are considered a possible source of MSCs. MSCs have great significance with regard to tissue homeostasis, and may additionally regulate inflammatory reactions, and stem cell renewal and induction. BM-MSCs are recognized as an ideal resource for use in stem cell therapy due to their multipotent differentiation capability, immunosuppressive function, rapid proliferative ability, abundance and their possible high degree of purification. It appears that the present study is the first to demonstrate that BM-MSCs derived from the Tibetan mastiff have stable genetic properties and multipotent differentiation capability. In future, studies may focus on the underlying molecular mechanisms of hepatocyte-like cell differentiation and compare Tibetan mastiff BM-MSCs with those derived from other species.

To examine the potential multipotent differentiation of BM-MSCs, it was determined whether BM-MSCs may be

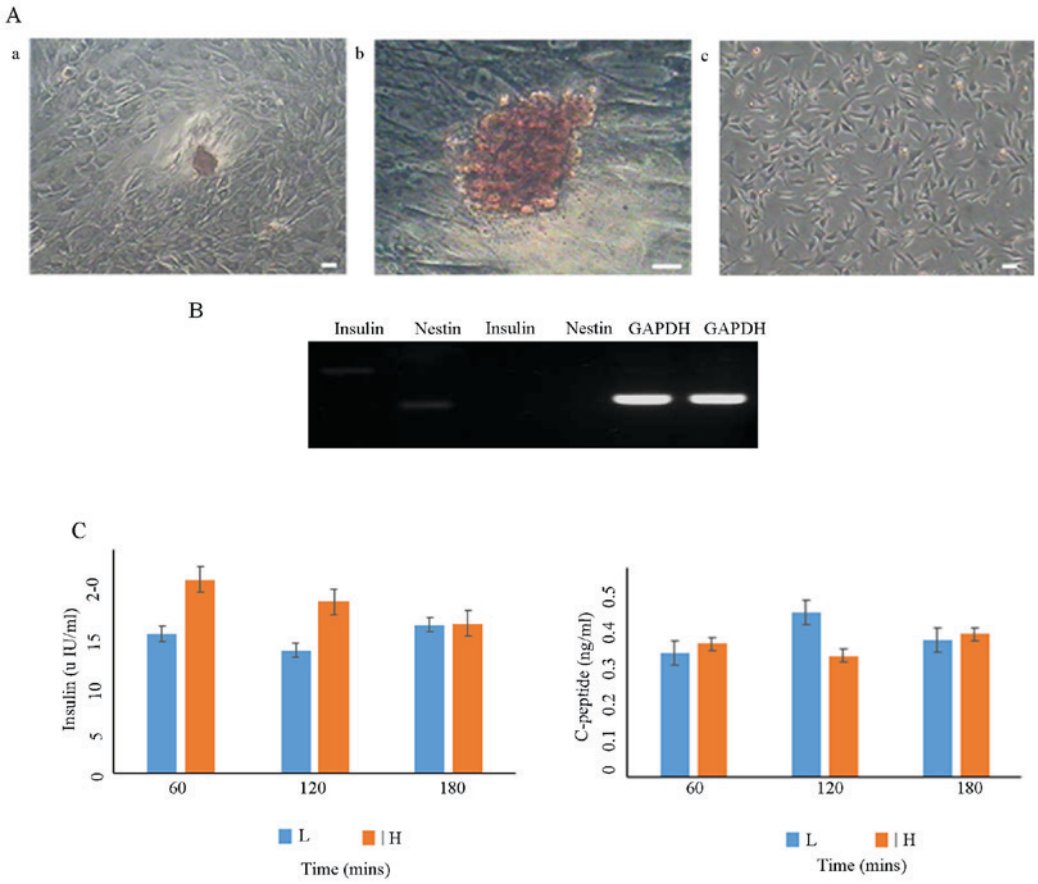

Figure 11. Functional insulin-producing β-like cell differentiation. (A) Following induction, BM-MSCs formed obvious islet-like clusters. All clusters were stained scarlet with dithizone (scale bar=100 μm): (a) magnification, x40, (b) magnification, x200 and (c) control group cells without staining (magnification, x40). (B) Semi-quantitative polymerase chain reaction analysis demonstrated that the induced group expressed the islet cell-specific genes INS and NES; however, the control group did not express these genes. (C) ELISA measurement of insulin and C-peptide at different concentrations of glucose. Data are presented as the mean ± standard deviation. BM-MSCs, bone marrow mesenchymal stem cells; INS, insulin; NES, nestin.

successfully induced to differentiate into osteocytes, adipocytes, chondrocytes, hepatocyte-like cells and insulin-secreting cells. Cells cultured in each of the different inducing media exhibited notable staining and gene expression differences compared with the non-induced (control) cells.

The adipogenic induction medium included dexamethasone, insulin and isobutyl methylxanthine. Dexamethasone is a corticosteroid medication that may control immune and metabolic reactions. During differentiation, dexamethasone increases gene transcription and interferes with the Wnt signaling pathway. Insulin, a peptide hormone, controls fat metabolism, whereas isobutyl methylxanthine is a phosphodiesterase inhibitor and stimulates the synthesis of cyclic adenosine monophosphate. All three factors combined may successfully induce adipogenic differentiation. These adipogenic stimuli activate PPAR-γ to terminate the induction of pre-adipocytes. The co-existence of PPAR-γ and LPL may lead to the expression of adipocyte genes including LPL and PPAR-γ (34).

L-ascorbic acid, dexamethasone and β-glycerophosphate may maintain the morphology of osteogenic induced cells, which alter from spindle-shaped cells into diamond-shaped osteoblasts. Notch, Wnt and bone morphogenetic protein may regulate osteogenic induction (35), providing a basis for determining the underlying mechanism of osteogenic induction.

In the present study, chondrogenic induction of BM-MSCs led to cluster-like aggregation. Alcian blue staining and semi-quantitative PCR for COL2A1 and SOX9 gene expression were used to determine successful induction. Activation of the mitogen-activated protein kinase P38 pathway may induce chondrogenic differentiation of BM-MSCs (36).

To assess the functional differentiation of BM-MSCs into hepatocyte-like cells, the present study evaluated the induction rate by flow cytometry, ALB expression by immunofluorescence staining, glycogen levels by periodic acid-Schiff staining and the expression of ALB and AFP by semi-quantitative-PCR. It was revealed that BM-MSCs were induced into hepatocyte-like cells successfully with a one-step protocol. For the induction medium, fibroblast growth factor (FGF)-4, HGF, ITS and dexamethasone were added. HGF is a cytokine that is secreted by sinusoidal endothelial cells and Kupffer cells and stimulates the proliferation of hepatocytes. FGF-4 may promote the development and growth of the fetal liver and is a signaling molecule originating in the endoderm layer, whereas ITS and dexamethasone may stimulate hepatocyte nuclear factor 4, an important transcription factor, thereby inducing the differentiation and maturation of hepatocytes. However, these mechanisms are not well understood at present, and it is necessary to further investigate methods of induction. More extensive research is required to examine the signaling

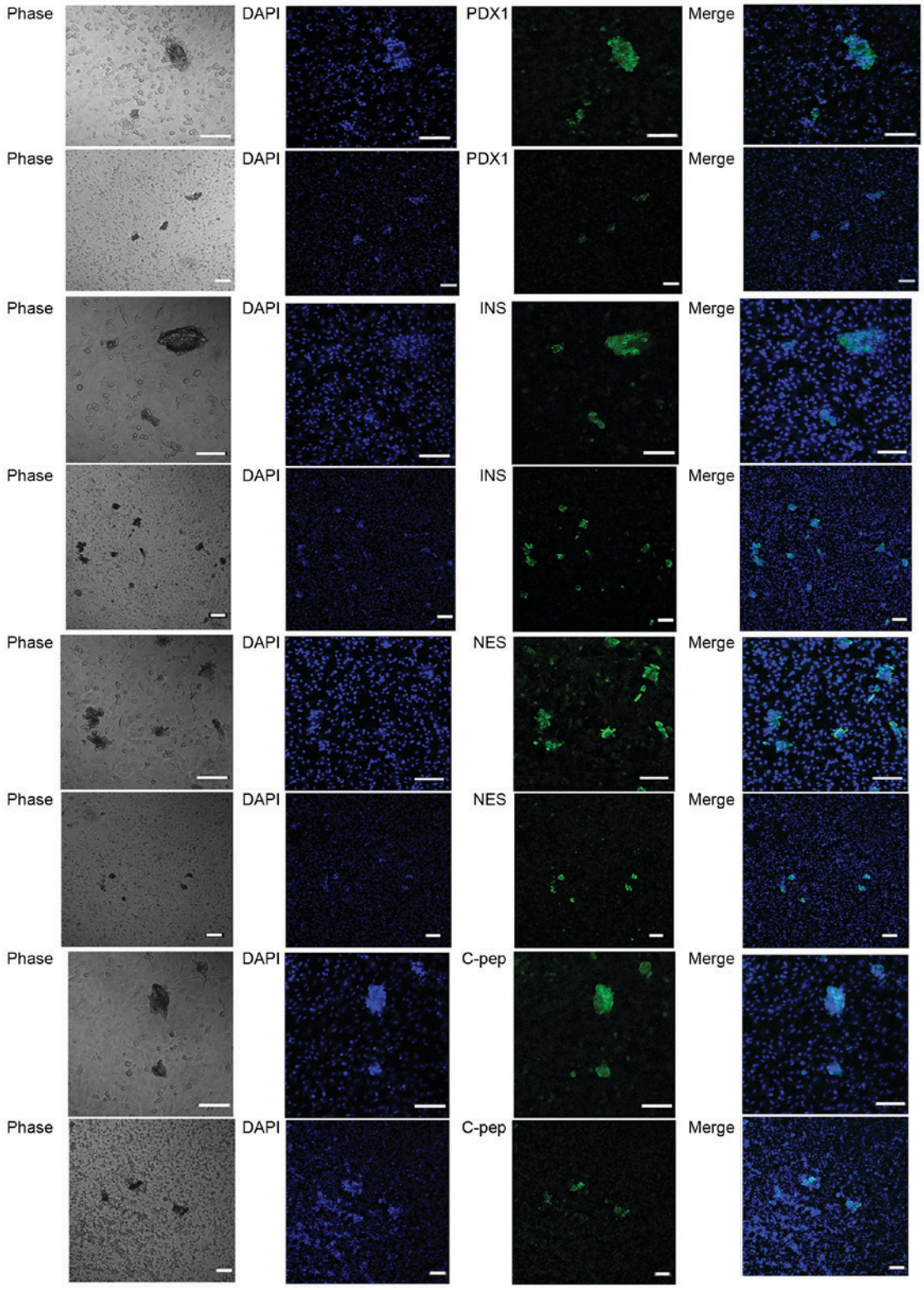

Figure 12. Immunofluorescence analysis of insulin-producing β-like cell differentiation. Islet-like cell clusters expressed PDX-1, INS, NES and C-peptide (C-Pep). Nuclear staining was performed with DAPI (scale bar=50 μm). INS, insulin; NES, nestin; C-Pep, C-peptide; PDX-1, pancreatic and duodenal homeobox 1.

pathways involved in induction, and this may have important implications for the treatment of liver injury.

To assess the functional differentiation of BM-MSCs into insulin-secreting cells, the secretion of insulin in response to different concentrations of glucose was determined using ELISA, the expression of C-peptide, insulin, nestin and PDX-1 was determined by immunofluorescence, the presence of islet-like clusters was ascertained by dithizone staining, and INS and NES expression levels were determined by semi-quantitative PCR. To induce the differentiation of BM-MSCs into insulin-secreting cells, a three-step protocol was used including only a defined media and no transfection.

This approach was chosen for its potential therapeutic applications. In the third step, exendin-4 and activin A maintained increased expression of β-cell markers. Replication and neogenesis of β-cells are stimulated by exendin-4, which is a potent glucagon-like peptide-1 agonist (37). Although the present study was able to induce differentiation into insulin-secreting cells and verify the function of these cells *in vitro*, the underlying mechanism is not completely understood. In order to test the applicability of this method for the treatment of diabetes, it is necessary to explore the cell signaling pathways involved in induction and demonstrate their functionality in future *in vitro* and *in vivo* studies.

In conclusion, the findings of the present study preliminarily verified that Tibetan mastiff-derived BM-MSCs are a potential resource for clinical applications, including cell therapy and tissue engineering. However, the underlying mechanisms of the differentiation of these cells remain to be elucidated and determining these mechanisms is essential, as they may be associated with certain mechanisms of tissue repair. Further work is required to focus on the ability of Tibetan mastiff-derived BM-MSCs to treat associated diseases in animal models, in addition to the underlying molecular mechanisms and signaling pathways. The present study revealed that BM-MSCs were derived from the Tibetan mastiff, and the self-renewal capability and functional differentiation of these cells were verified *in vitro*. The present study further proved the regenerative ability of Tibetan mastiff-derived BM-MSCs, and revealed that the bone marrow is a potential source of progenitor cells for the treatment of various canine diseases.

Acknowledgements

The authors would like to thank Mr. Wenhua Pei (Institute of Animal Science, Chinese Academy of Agricultural Sciences, Beijing, China) for supplying cell factors and Mr. Tengfei Lu (Institute of Animal Science, Chinese Academy of Agricultural Sciences, Beijing, China) for providing trypsin.

Funding

The present study was supported by a grant from the Agricultural Science and Technology Innovation Program (grant no. cxgc-ias-01), the National Natural Science Foundation of China (grant nos. 31472099 and 31672404) and the School Subject of Harbin Sport University (grant no. 2017 TJ 009).

Availability of data and materials

All data generated or analyzed during the present study are included in this published article.

Authors' contributions

SZ and CZ designed and coordinated the study. YW contributed to the isolation and chondrogenic differentiation of BM-MSCs. SL performed the analysis of chromosome and karyotype. YZ contributed to figure preparation. ZZ designed and supervised the study. WG provided the study materials and analyzed the data.

Ethics approval and consent to participate

The present study was approved by the Institute of Animal Science, Chinese Academy of Agricultural Sciences (Beijing, China).

Consent for publication

Not applicable.

Competing interests

The authors declare that they have no competing interests.

References

1. Cristancho AG and Lazar MA: Forming functional fat: A growing understanding of adipocyte differentiation. Nat Rev Mol Cell Biol 12: 722-734, 2011.
2. De Coppi P, Bartsch G Jr., Siddiqui MM, Xu T, Santos CC, Perin L, Mostoslavsky G, Serre AC, Snyder EY, Yoo JJ, *et al*: Isolation of amniotic stem cell lines with potential for therapy. Nat Biotechnol 25: 100-106, 2007.
3. Pozzobon M, Piccoli M, Schiavo AA, Atala A and De Coppi P: Isolation of c-Kit+ human amniotic fluid stem cells from second trimester. Methods Mol Biol 1035: 191-198, 2013.
4. Kinnaird T, Stabile E, Burnett MS, Lee CW, Barr S, Fuchs S and Epstein SE: Marrow-derived stromal cells express genes encoding a broad spectrum of arteriogenic cytokines and promote in vitro and in vivo arteriogenesis through paracrine mechanisms. Circ Res 94: 678-685, 2004.
5. da Silva Meirelles L, Caplan AI and Nardi NB: In search of the in vivo identity of mesenchymal stem cells. Stem Cells 26: 2287-2299, 2008.
6. Beyer Nardi N and da Silva Meirelles L: Mesenchymal stem cells: Isolation, in vitro expansion and characterization. Handb Exp Pharmacol: 249-282, 2006.
7. Deans RJ and Moseley AB: Mesenchymal stem cells: Biology and potential clinical uses. Exp Hematol 28: 875-884, 2000.
8. Sanchez-Ramos J, Song S, Cardozo-Pelaez F, Hazzi C, Stedeford T, Willing A, Freeman TB, Saporta S, Janssen W, Patel N, *et al*: Adult bone marrow stromal cells differentiate into neural cells in vitro. Exp Neurol 164: 247-256, 2000.
9. McLean K, Gong Y, Choi Y, Deng N, Yang K, Bai S, Cabrera L, Keller E, McCauley L, Cho KR and Buckanovich RJ: Human ovarian carcinoma-associated mesenchymal stem cells regulate cancer stem cells and tumorigenesis via altered BMP production. J Clin Invest 121: 3206-3219, 2011.
10. Yang X, Hou J, Han Z, Wang Y, Hao C, Wei L and Shi Y: One cell, multiple roles: Contribution of mesenchymal stem cells to tumor development in tumor microenvironment. Cell Biosci 3: 5, 2013.
11. Chen S, Wang L, Fan J, Ye C, Dominguez D, Zhang Y, Curiel TJ, Fang D, Kuzel TM and Zhang B: Host miR155 promotes tumor growth through a myeloid-derived suppressor cell-dependent mechanism. Cancer Res 75: 519-531, 2015.
12. Wang J, Yu F, Jia X, Iwanowycz S, Wang Y, Huang S, Ai W and Fan D: MicroRNA-155 deficiency enhances the recruitment and functions of myeloid-derived suppressor cells in tumor microenvironment and promotes solid tumor growth. Int J Cancer 136: E602-E613, 2015.
13. Ward CL, Sanchez CJ Jr, Pollot BE, Romano DR, Hardy SK, Becerra SC, Rathbone CR and Wenke JC: Soluble factors from biofilms of wound pathogens modulate human bone marrow-derived stromal cell differentiation, migration, angiogenesis, and cytokine secretion. BMC Microbiol 15: 75, 2015.
14. Zhang D, Liu X, Peng J, He D, Lin T, Zhu J, Li X, Zhang Y and Wei G: Potential spermatogenesis recovery with bone marrow mesenchymal stem cells in an azoospermic rat model. Int J Mol Sci 15: 13151-13165, 2014.
15. Tan SL, Ahmad TS, Selvaratnam L and Kamarul T: Isolation, characterization and the multi-lineage differentiation potential of rabbit bone marrow-derived mesenchymal stem cells. J Anat 222: 437-450, 2013.

16. Adamzyk C, Kachel P, Hoss M, Gremse F, Modabber A, Holzle F, Tolba R, Neuss S and Lethaus B: Bone tissue engineering using polyetherketoneketone scaffolds combined with autologous mesenchymal stem cells in a sheep calvarial defect model. J Craniomaxillofac Surg 44: 985-994, 2016.
17. Kocamaz E, Gok D, Cetinkaya A and Tufan AC: Implication of C-type natriuretic peptide-3 signaling in glycosaminoglycan synthesis and chondrocyte hypertrophy during TGF-beta1 induced chondrogenic differentiation of chicken bone marrow-derived mesenchymal stem cells. J Mol Histol 43: 497-508, 2012.
18. Ramírez-Espinosa JJ, González-Dávalos L, Shimada A, Piña E, Varela-Echavarria A and Mora O: Bovine (bos taurus) bone marrow mesenchymal cell differentiation to adipogenic and myogenic lineages. Cells Tissues Organs 201: 51-64, 2016.
19. Wang M, Wang YH, Ye Q, Meng P, Yin H and Zhang DL: Serological survey of toxoplasma gondii in tibetan mastiffs (*canis lupus familiaris*) and yaks (*Bos grunniens*) in Qinghai, China. Parasit Vectors 5: 35, 2012.
20. Messerschmidt GL, Bowles C, Alsaker R, McCormack K, Corbitt RH, Mosley KR and Deisseroth AB: Prognostic indicators of tumor response to Staphylococcus aureus Cowan strain I plasma perfusion. J Natl Cancer Inst 71: 535-538, 1983.
21. Cui Y, Guo W, Li D, Wang L, Shi CX, Brookmeyer R, Detels R, Ge L, Ding Z and Wu Z: Estimating HIV incidence among key affected populations in China from serial cross-sectional surveys in 2010-2014. J Int AIDS Soc 19: 20609, 2016.
22. Li Q, Liu Z, Li Y, Zhao X, Dong L, Pan Z, Sun Y, Li N, Xu Y and Xie Z: Origin and phylogenetic analysis of tibetan mastiff based on the mitochondrial DNA sequence. J Genet Genomics 35: 335-340, 2008.
23. Kijas JW, Miller BJ, Pearce-Kelling SE, Aguirre GD and Acland GM: Canine models of ocular disease: Outcross breedings define a dominant disorder present in the English mastiff and bull mastiff dog breeds. J Hered 94: 27-30, 2003.
24. Huang B, Cheng X, Wang H, Huang W, la Ga Hu Z, Wang D, Zhang K, Zhang H, Xue Z and Da Y: Mesenchymal stem cells and their secreted molecules predominantly ameliorate fulminant hepatic failure and chronic liver fibrosis in mice respectively. J Transl Med 14: 45, 2016.
25. Chouinard L, Martineau D, Forget C and Girard C: Use of polymerase chain reaction and immunohistochemistry for detection of canine adenovirus type 1 in formalin-fixed, paraffin-embedded liver of dogs with chronic hepatitis or cirrhosis. J Vet Diagn Invest 10: 320-325, 1998.
26. Nagamoto Y, Takayama K, Ohashi K, Okamoto R, Sakurai F, Tachibana M, Kawabata K and Mizuguchi H: Transplantation of a human iPSC-derived hepatocyte sheet increases survival in mice with acute liver failure. J Hepatol 64: 1068-1075, 2016.
27. Li LH, Zhao YY and Wu XG: Progress in the study of diabetes in dogs. China Vet J 8: 64-65, 2008.
28. Samarghandian S, Azimi-Nezhad M, Samini F and Farkhondeh T: Chrysin treatment improves diabetes and its complications in liver, brain, and pancreas in streptozotocin-induced diabetic rats. Can J Physiol Pharmacol 94: 388-393, 2016.
29. Chaiyasut C, Kusirisin W, Lailerd N, Lerttrakarnnon P, Suttajit M and Srichairatanakool S: Effects of phenolic compounds of fermented thai indigenous plants on oxidative stress in streptozotocin-induced diabetic rats. Evid Based Complement Alternat Med 2011: 749307, 2011.
30. Motta-Silva AC, Aleva NA, Chavasco JK, Armond MC, Franca JP and Pereira LJ: Erythematous oral candidiasis in patients with controlled type II diabetes mellitus and complete dentures. Mycopathologia 169: 215-223, 2010.
31. Bai C, Chen S, Gao Y, Shan Z, Guan W and Ma Y: Multi-lineage potential research of bone marrow mesenchymal stem cells from Bama miniature pig. J Exp Zool B Mol Dev Evol 324: 671-685, 2015.
32. Anjos-Afonso F and Bonnet D: Isolation, culture, and differentiation potential of mouse marrow stromal cells. Curr Protoc Stem Cell Biol Chapter 2:Unit 2B.3, 2008.
33. Majumdar MK, Banks V, Peluso DP and Morris EA: Isolation, characterization, and chondrogenic potential of human bone marrow-derived multipotential stromal cells. J Cell Physiol 185: 98-106, 2000.
34. Reyes M, Lund T, Lenvik T, Aguiar D, Koodie L and Verfaillie CM: Purification and ex vivo expansion of postnatal human marrow mesodermal progenitor cells. Blood 98: 2615-2625, 2001.
35. Zhang S, Bai CY, Ma YH, Li XC, Gao YH, Fan YN, Wei JG and Zheng D: The characterisation and functional β-cell differentiation of duck pancreas-derived mesenchymal cells. Br Poult Sci 57: 201-210, 2016.
36. Lv FJ, Tuan RS, Cheung KM and Leung VY: Concise review: The surface markers and identity of human mesenchymal stem cells. Stem Cells 32: 1408-1419, 2014.
37. Noort WA, Oerlemans MI, Rozemuller H, Feyen D, Jaksani S, Stecher D, Naaijkens B, Martens AC, Bühring HJ, Doevendans PA and Sluijter JP: Human versus porcine mesenchymal stromal cells: Phenotype, differentiation potential, immunomodulation and cardiac improvement after transplantation. J Cell Mol Med 2012, 16:1827-1839.